Author(s): Ahokas, Jussi; Kosendiak, Iwona; Krupa, Justyna; Lundell, Jan; Wierzejewska, Maria

Title: FTIR matrix isolation and theoretical studies of glycolic acid dimers

Year: 2018

Version:

Please cite the original version:

Ahokas, J., Kosendiak, I., Krupa, J., Lundell, J., & Wierzejewska, M. (2018). FTIR matrix isolation and theoretical studies of glycolic acid dimers. Journal of Molecular Structure, 1163, 294-299. https://doi.org/10.1016/j.molstruc.2018.03.019

Accepted Manuscript

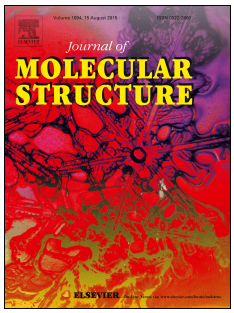

FTIR matrix isolation and theoretical studies of glycolic acid dimers

Jussi Ahokas, Iwona Kosendiak, Justyna Krupa, Jan Lundell, Maria Wierzejewska

PII: S0022-2860(18)30302-8

DOI: 10.1016/j.molstruc.2018.03.019

Reference: MOLSTR 24958

To appear in: *Journal of Molecular Structure*

Received Date: 13 December 2017

Revised Date: 5 March 2018

Accepted Date: 6 March 2018

Please cite this article as: J. Ahokas, I. Kosendiak, J. Krupa, J. Lundell, M. Wierzejewska, FTIR matrix isolation and theoretical studies of glycolic acid dimers, *Journal of Molecular Structure* (2018), doi: 10.1016/j.molstruc.2018.03.019.

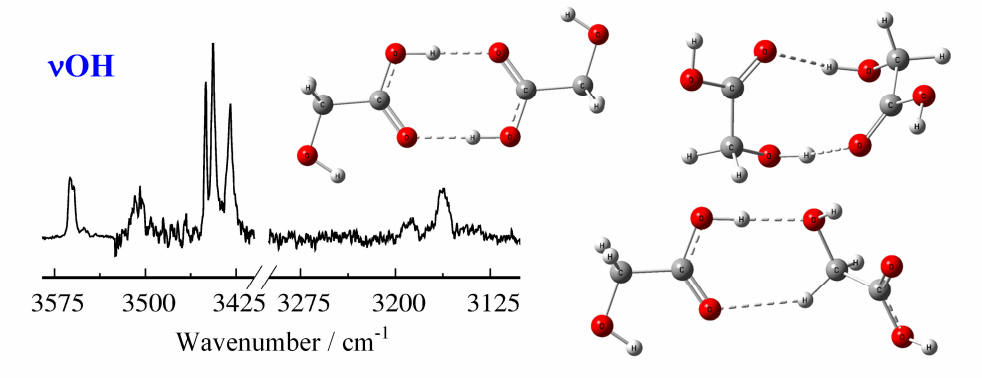

FTIR Matrix Isolation and Theoretical Studies of Glycolic Acid Dimers

Jussi Ahokas[1*], Iwona Kosendiak[2], Justyna Krupa[2], Jan Lundell[3], Maria Wierzejewska[2*]

[1]Nanoscience Center, Department of Chemistry, University of Jyväskylä, FI-40014 Jyväskylä, Finland
[2]Faculty of Chemistry, University of Wrocław, Joliot-Curie 14, 50-383 Wrocław, Poland
[3]Department of Chemistry, University of Jyväskylä, FI-40014 Jyväskylä, Finland

Abstract

Glycolic acid (GA) dimers were studied in low temperature argon matrices by means of FTIR spectroscopy. Experimentally, the dimers were produced when monomeric glycolic acid molecules were thermally mobilized upon annealing of argon matrices at 25-35 K. The experimental spectra observed upon annealing indicate the presence of three different dimer structures. Computationally, MP2 and DFT calculations were used to study the potential dimer species in order to scrutinize the possible dimer structures, their energetics and their spectral features. Altogether 27 local minima were found for dimer structures for the three lowest conformers of glycolic acid considered based on previous studies on glycolic monomer in argon matrices. Comparing the computational and the experimental spectra especially in the O-H and C=O stretching regions it was possible to assign the experimental observations to the three most stable dimer species.

*- corresponding authors: e-mails addresses: jussi.m.e.ahokas@jyu.fi (J. A.)
maria.wierzejewska@chem.uni.wroc.pl (M.W.)

1. Introduction

Hydrogen bonding as one of the strongest intermolecular interactions plays an important role in many chemical and biological processes. Hydrogen bonded complexes have also a significant influence on the atmospheric chemistry and are considered to contribute to chemistry of interstellar media and planetary atmospheres [1-3]. Among many important hydrogen bonded species carboxylic acid dimers have been extensively studied both theoretically and experimentally [4-9]. Carboxylic acids form in the gas phase very stable cyclic dimers with two equivalent O-H···O bridges. In the solid state both cyclic structures (dimers) and infinite chains with monomers joined by hydrogen bonds are observed [10-16].

Monomeric glycolic acid (GA), the smallest of the α-hydroxy carboxylic acids, has been studied in the gas phase [17-20], low temperature matrices [21-25] and in supersonic expansion [26]. The crystal structure of GA is made up of chains and no isolated cyclic dimers are found. The GA molecules are linked by hydrogen bonds formed between carboxylic groups as proton donors and hydroxylic oxygen atoms as proton acceptors. The geometry of the individual GA molecules in the crystal resembles that of the SSC (*syn-syn-cis*) conformer observed in the gas phase with the alcohol OH group slightly deviated from the molecular plane.

According to theoretical predictions [20,21,24] the SSC conformer (see Fig. 1) is a global minimum on the potential energy surface of GA. All available experimental data confirm that SSC is the most populated form of the compound. The relative abundancy of the most stable monomeric form SSC is *ca.* 95% at room temperature [23]. In addition to SSC only small amounts of two less stable isomers: AAT (*anti-anti-trans*) and GAC (*gauche-anti-cis*) were found in jets [26] and in low temperature matrices [21-25].

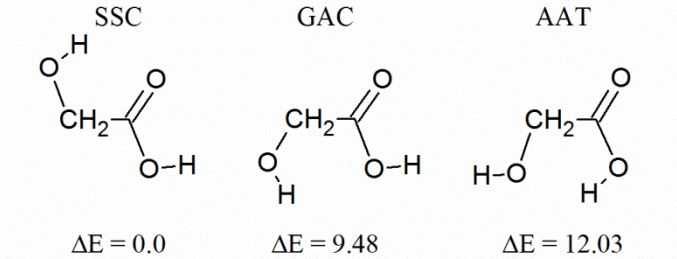

Fig. 1. Schematic representation of three most stable conformers of glycolic acid monomer. Relative energies ΔE obtained at MP2/aug-cc-pVDZ are given in kJ mol^{-1} [24].

In this paper we present results of experimental and theoretical studies of glycolic acid dimers. Matrix isolation (MI) coupled with FTIR spectroscopy was applied which is an established technique for studying small hydrogen bonded systems [27-29]. When supported with computational methods the isolated hydrogen bonded complex structures are well resolved and distinguishable.

2. Experimental and computational details

The matrix samples were prepared by passing high purity argon (Messer, 5.0) through the glass U-tube with glycolic acid (GA) situated outside the cryostat chamber. The matrix-to-sample ratio could not be precisely determined, but matrices containing dimeric GA species could be obtained by optimizing the deposition temperature and the gas flow rate (2 mbar per minute). The GA/Ar gaseous mixtures were deposited onto a cold CsI window kept at 15 K, 18 K or 25 K by a closed cycle cryostat APD-Cryogenics (ARS-2HW). Annealing experiments were performed upon the deposited samples at 25, 27, 30, 33, and 35 K. Sample temperature was maintained by a Scientific Instruments 9700 temperature controller equipped with a silicon diode and a resistive heater. Infrared spectra were recorded in a transmission mode with a 0.5 cm^{-1} resolution using a purged Bruker IFS 66 Fourier Transform spectrometer equipped with a liquid N_2 cooled MCT detector.

All calculations were carried out using the Gaussian09 program package [30]. For all types of dimers (SSC-SSC, SSC-GAC, SSC-AAT, GAC-GAC, AAT-AAT) MP2/6-

311++G(2d,2p) [31-35] calculations were performed. The SSC-SSC dimers were additionally studied at the B3LYP, B3LYPD3 and B2PLYPD3 levels [36-42] of theory in order to assess their performance compared to the MP2 calculations. The obtained energies of the dimers were corrected for basis set superposition error (BSSE) by the Boys-Bernardi full counterpoise method [43]. The topological analysis of the electron density (AIM) [44] has been performed at the MP2 level using AIM program as implemented in Gaussian09. The harmonic vibrational wavenumbers and intensities were calculated at all four levels for the optimized dimer structures to assist the analysis of the experimental spectra. In the next sections the MP2 energies will be used, unless otherwise indicated. During the study it was found that MP2 and DFT calculations yield very similar structural parameters and identical energy orders between complex structures. On the other hand, the B3LYP wavenumbers were used for the purpose of discussion due to their best fit to the experimental findings, as the MP2 computed vibrational wavenumbers showed irregular performance for different complex structures. The actual origin of this observation is still unclear and more elaborate computational studies are underway beyond harmonic approach to investigate this issue further. The B3LYP/6-311++G(2d,2p) wavenumbers of the SSC-SSC dimers scaled by 0.9506, above 2500 cm^{-1}, and by 0.9845, in the 2500−500 cm^{-1} spectral region, were used to simulate their infrared spectra. The scaling factors were obtained from fitting the computed vibrational wavenumbers with respect to the observed vibrational band positions.

3. Results and discussion

3.1. Computational results

Since three monomeric GA isomers SSC, GAC and AAT (see Fig. 1) were detected in argon matrices [21,22,24] the calculations have been performed for the following dimers: SSC-SSC, SSC-GAC, SSC-AAT, GAC-GAC, AAT-AAT. For these dimers altogether 27

local minima were found at all levels of theory. The eight SSC-SSC stable structures (further denoted as dSSn, n = 1-8) are presented in Fig. 2 whereas all remaining dimer species are shown in Fig. S1 in Supplementary data. The calculated geometric parameters of dSSn dimers are gathered in Table S1. Four of these structures are linked by two (dSS1, dSS2, dSS6 and dSS7) or one (dSS4) hydrogen bonds of the O-H···O type. In two other species (dSS3 and dSS5) the moieties are joined by one O-H···O and one C-H···O bonds. The binding forces in the (dSS8) dimer are two C-H···O interactions. Table 1 presents the calculated values of the intermolecular parameters obtained for dSSn dimers as well as two topological parameters obtained from Bader's quantum Theory of Atoms in Molecules [44].

Table 1. Interatomic distances (Å), angles (degree) and electron density parameters of the intermolecular bond critical points (au) of the glycolic acid dimers computed at MP2/6-311++G(2d,2p) level.

Dimer		Intermolecular parameters[a]			AIM parameters	
		Distances		Angle	ρ(r)	$\nabla^2\rho(r)$
		H···O	X···O	N–H···Y		
dSS1	O-H···O	1.744	2.731	179.3	0.038	0.111
	O-H···O	1.744	2.731	179.3	0.038	0.111
dSS2	O-H···O	2.023	2.908	151.3	0.021	0.073
	O-H···O	2.024	2.909	151.3	0.021	0.073
dSS3	O-H···O	1.777	2.761	179.2	0.036	0.106
	C-H···O	2.402	3.286	137.4	0.011	0.036
dSS4	O-H···O	1.801	2.756	163.6	0.033	0.106
dSS5	O-H···O	1.894	2.863	179.7	0.027	0.090
	C-H···O	2.615	3.148	109.4	0.008	0.028
dSS6	O-H···O	1.905	2.866	179.3	0.027	0.088
	O-H···O	2.170	2.898	130.8	0.015	0.058
dSS7	O-H···O	2.053	2.941	151.1	0.017	0.067
	O-H···O	1.976	2.768	136.5	0.024	0.084
dSS8	C-H···O	2.435	3.400	147.0	0.010	0.033
	C-H···O	2.434	3.399	147.1	0.010	0.033

[a] X is O or C atom

Table 2. Computed BSSE corrected interaction energies (in kJ mol^{-1}) of eight dSSn dimers.

Dimer	MP2	B3LYP	B3LYPD3	B2PLYPD3
dSS1	-64.64	-71.96	-83.39	-76.02
dSS2	-53.14	-46.02	-64.22	-58.24
dSS3	-41.21	-38.83	-49.08	-45.61
dSS4	-35.23	-32.38	-42.17	-38.70
dSS5	-30.75	-26.48	-37.66	-34.35
dSS6	-29.46	-26.48	-38.74	-33.76
dSS7	-28.20	-26.78	-35.31	-32.30
dSS8	-15.02	-9.96	-18.79	-16.40

The computed interaction energies are presented in Table 2, whereas the relative energies are given in Table S2. For the four most stable dimer species the interaction energy order is identical at all four levels of theory and the same is true for the overall geometry of these structures. The most stable species with the interaction energy of -64.64 kJ mol^{-1} at the MP2 level is dSS1 comprising an eight-member ring formed between carboxylic groups bonded by two O-H···O hydrogen bonds with the H···O intermolecular distance of 1.744 Å each. The second dimer as to the interaction energy (-53.14 kJ mol^{-1}) is dSS2 with two O-H···O hydrogen bonds between the alcohol OH groups and carbonyl oxygen atoms and ten-member ring present. In other cases six-, seven- or eight- membered rings are noticeable with the intermolecular H···O distances in the range of 1.8-2.4 Å and 2.4-2.6 Å for the O-H···O and C-H···O hydrogen bonds, respectively. The third structure is dSS3 (E_{int}=-41.21 kJ mol^{-1}) characterized by one O-H···O bond formed between carboxylic hydroxyl group and the oxygen atom of another OH group. The performed AIM calculations revealed additional interaction within the dSS3 dimer of the C-H···O type which has its important contribution to the relatively high stability of this species. For the less stable dSSn dimer structures the computed interaction energies at MP2 range between -15.02 and -35.23 kJ mol^{-1}. Among

them the least stable is dSS8 that does not comprise any O-H···O bond and the moieties are connected by two C-H···O interactions characterized by relatively long H···O distances with non-linear C···O bridges (see Table 1).

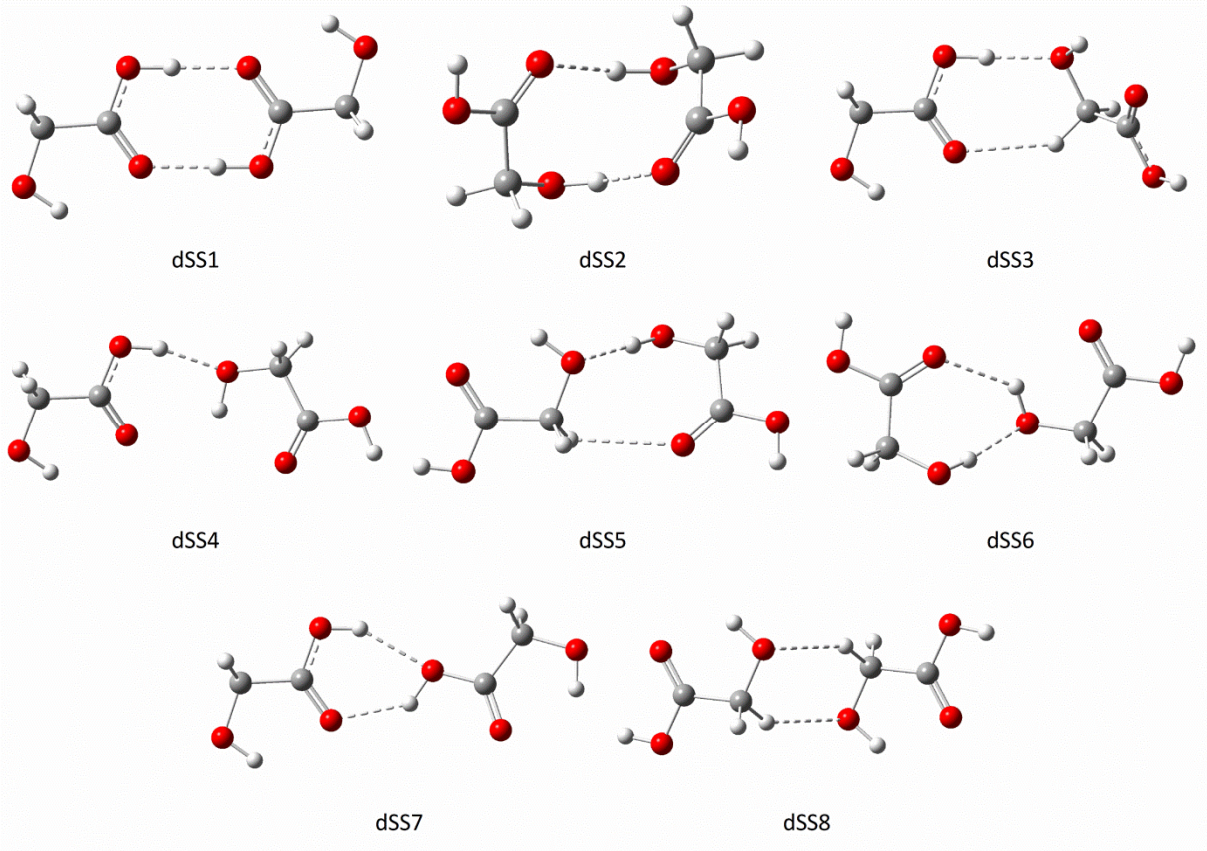

Fig. 2. MP2/6-311++G(2d,2p) optimized dSSn structures of glycolic acid dimer. The dashed lines indicate interactions between subunits as evidenced by AIM.

3.2.Experimental spectra of GA dimers in argon matrices and their analysis

The vibrational spectrum of monomeric glycolic acid was recorded at 10 K after the deposition of a gaseous mixture containing glycolic acid and argon onto a CsI substrate kept at 18 K. The most characteristic bands of GA monomer were observed at 3561, 1806, 1783, 1773, 854, and 825 cm^{-1} (see trace a in Figs 3 and 4) in agreement with earlier studies [21,24]. In addition to the known monomer bands, a number of weaker bands was observed in the vicinity of the monomer absorptions. When the sample was annealed at higher temperatures, the growth of these weak absorptions was observed while the vibrational bands of the monomer significantly decreased. Traces b in Figs 3 and 4 show the νOH and νC=O

stretching regions of the IR spectrum after the final annealing at 35 K. The overlap of bands in these regions prevented straightforward analysis of the observed absorptions and therefore Gaussian functions were used to locate individual maxima and to determine their integrated areas.

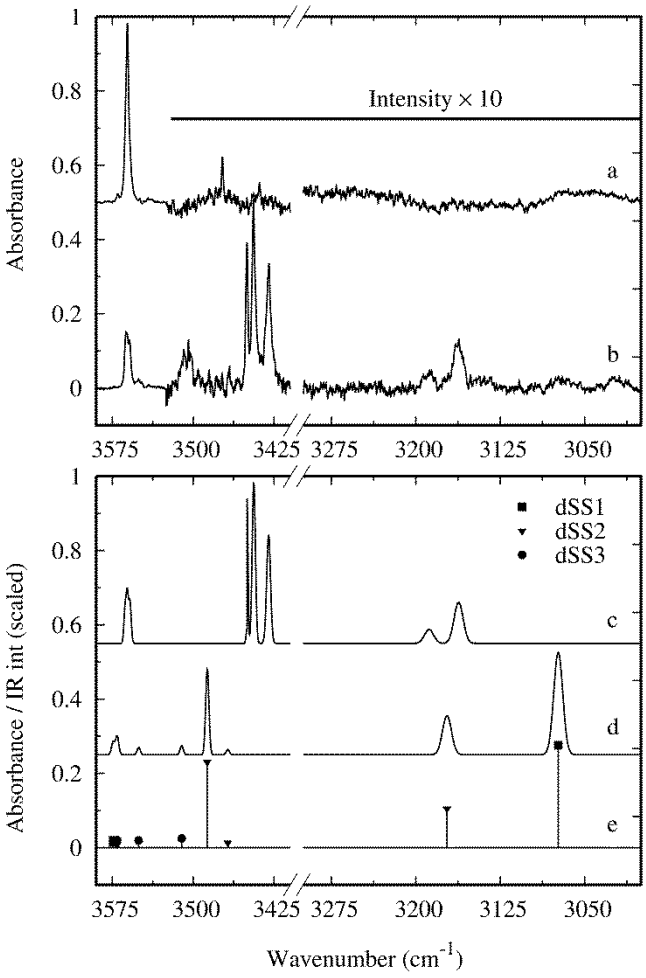

Fig. 3. The νOH stretching region. Upper graph: the FTIR spectra of GA in an argon matrix measured at 10 K: after deposition at 18 K (a) and after annealing at 35 K (b). Lower graph: the result of Gaussian fit of the Type 3 bands to the data (see text) (c), the computational IR sum spectrum of the dSS1, dSS2 and dSS3 conformers simulated with Gaussian functions (fwhm = 1.5 cm^{-1} in the 3300-3600 cm^{-1} region and fwhm = 4.0 cm^{-1} below 3300 cm^{-1}) (d) and theoretical stick spectra of the three dimers (e).

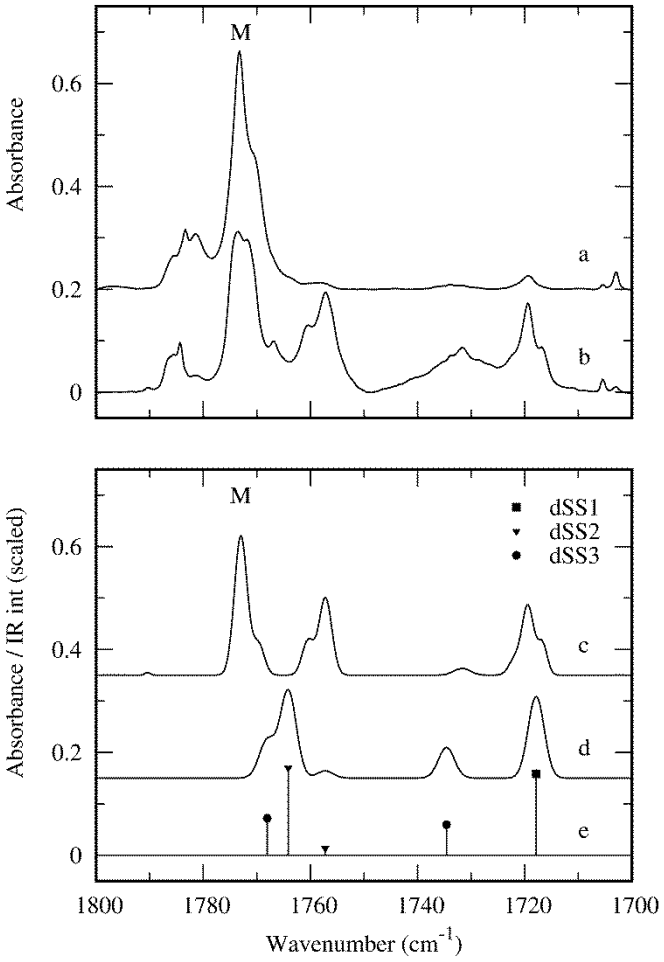

Fig. 4. The νC=O stretching region. Upper graph: the FTIR spectra of GA in an argon matrix measured at 10 K: after deposition at 18 K (a) and after annealing at 35 K (b). Lower graph: the result of Gaussian fit of the Type 3 bands to the data (see text) (c), the computational IR sum spectrum of the dSS1, dSS2 and dSS3 conformers simulated with Gaussian functions (fwhm = 1.5 cm^{-1}) (d) and theoretical stick spectra of the three dimers (e).

Fig. 5 shows the result of Gaussian fit to the data of the OH stretching region and the integrated absorbance of each observed band at the different annealing steps. The same analysis was carried out for the spectrum in the C=O stretching region. Three different annealing behaviors were extracted from these data. The monotonic decrease (Type 1) of the intensity was characteristic for the monomer bands in the OH and CO stretching regions. Two different kinds of growth in the populations of new species may be distinguished on the basis of the obtained annealing graphs. The first is monotonic growth (Type 3) while the second behavior (Type 2) is characterized by a milder growth and a significant drop in the population

during the last annealing step. The Type 2 absorbers have their bands close to the bands of GA monomer and typically, the intensities of Type 2 bands are weaker than those of the nearby monomer bands. A decrease of the relative population of the Type 2 absorbers is observed whereas negligible population changes at the same time of Type 3 and Type 1 absorbers is recorded.

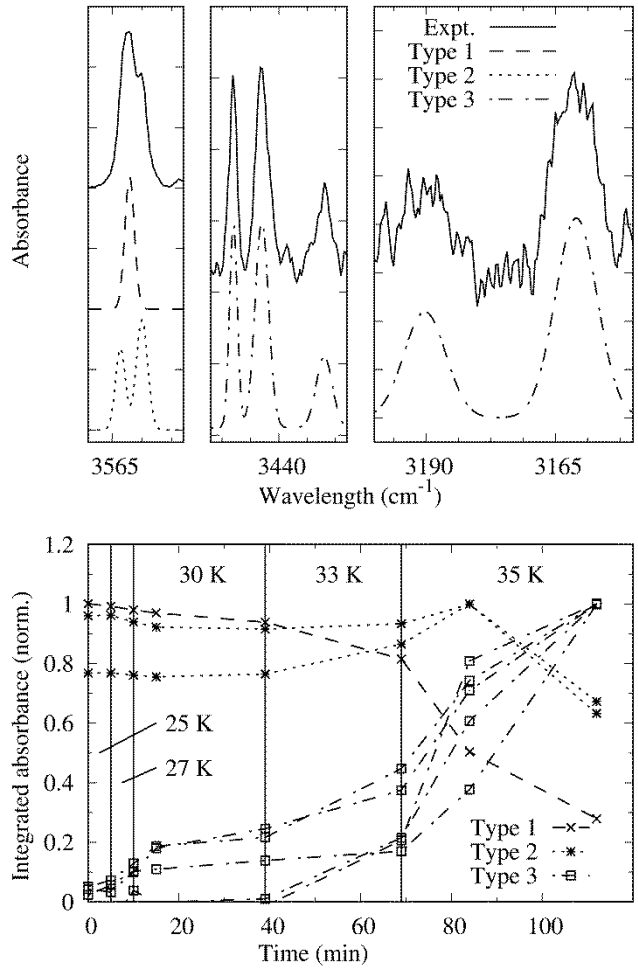

Fig. 5. Upper graph: the Gaussian functions used to fit experimental data in the OH stretching region. Types 1-3 stand for the three different kinds of annealing behavior of the observed absorbers. Lower graph: the normalized area used in the data fitting during the annealing. Vertical lines are used to separate the regions of the different annealing temperatures.

According to the above observations, the Type 2 absorbers may be considered as monomers in different sites and/or the monomers distorted by the intermolecular interactions of the molecules in neighboring trapping sites.

The Type 3 absorbers are the best candidates for the dimers due to their monotonic population increase. The validity of this assumption is supported by a linear dependence obtained for a plot of the normalized integrated absorbance of Type 1 bands versus the normalized integrated absorbance of bands of Type 3 (see Fig. 6). According to this linearity between the Types 1 and 3, the role of the Type 2 absorbers is negligible in the dimerization process. These assumptions were supported by experiments when the deposition temperature was varied. At higher deposition temperatures, the highest intensity bands of the Type 3 absorbers were already found after deposition. Unfortunately, the higher deposition temperature also favored the formation of higher aggregates and accordingly broad bands were present in the spectra. Some absorption bands of unstable dimer structures or unstable trapping sites of the dimer were also observed after the deposition at 25 K. These bands disappeared quickly at the lowest annealing temperatures and the conversion to more stable structures or trapping sites were observed. The more complex IR spectrum and annealing behavior of GA in an argon matrix at higher deposition temperatures led us to seek dimers by the annealing of matrices deposited at 18 K. The infrared spectrum of Type 3 absorbers is shown in Figs 3 and 4 (the top spectrum in the lower graph).

The annealing experiments here show that monomeric glycolic acid in an argon matrix undergoes efficient dimerization at annealing temperatures of 30 K or higher. The size of the GA monomer is sufficiently large to prevent a long-range thermal mobility at the deposition temperatures used in our experiments. Thus, one may assume relatively high monomeric GA concentration in the matrices. Therefore, the dimerization happens between the GA monomers in neighboring trapping sites.

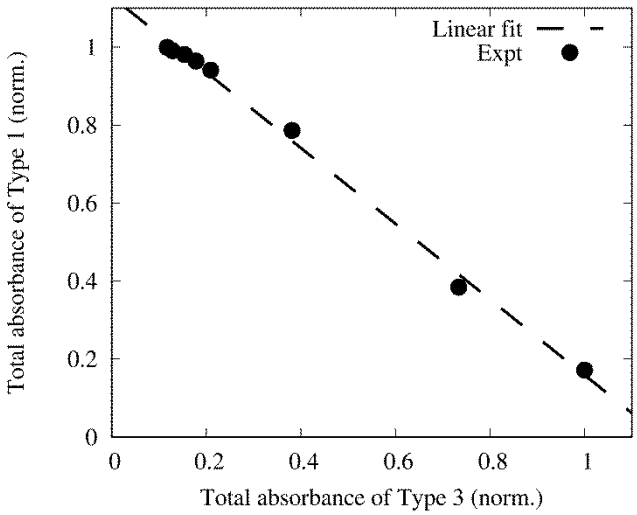

Fig. 6. The total absorbance of Type 1 (monomer) absorbers plotted against the total absorbance of Type 3 (dimers) absorbers. Dashed line demonstrates the linearity of the plot.

As the room temperature population of the SSC monomer is *ca.* 95%, it is reasonable to assume that the SSC dimers are the most probable dimer species trapped in low temperature matrices. The computational wavenumbers and intensities of three dSSn dimers (dSS1, dSS2 and dSS3) were used to simulate the IR sum spectrum that gives the best fit to the experimental spectra in the νOH and νC=O regions. This is shown as a middle trace in the lower graph of Figs 3 and 4. In addition, computational (stick) spectra of the individual dimers are also presented in the bottom part of Figs 3 and 4. The comparison of the Type 3 spectrum with computational spectrum shows apparent similarities.

Determination of the structures of the glycolic acid dimers present in the studied matrices was not an easy task. For proper choice of the dimer species for the spectra interpretation two criteria were taken into account. The first criterion was the interaction energy of the dimers and the second, equally important factor, was the calculated spectral characteristics of the dimeric forms. The best fit between theoretical and experimental spectra was obtained for B3LYP calculations and these data were used for the analysis. On the basis of the mentioned criteria the three most stable dimer structures (dSS1, dSS2, dSS3) have been chosen for the interpretation of the spectra after annealing (see Figs 3 and 4).

The most informative for the analysis is the OH stretching region of the spectra (Fig. 3). One can readily notice that there are two separate regions where the dimer bands appear. The doublet observed at 3188 and 3162 cm^{-1} is red shifted by -373 and -399 cm^{-1} relative to the νOH band of SSC monomer (3561 cm^{-1}, two overlapping bands due to the carboxylic and alcohol hydroxyl groups). According to the performed calculations there are two dimer structures, namely dSS1 and dSS3, that are characterized by the νOH shifts of the same order of magnitude. In both cases the shifts are those of the carboxylic OH groups involved in hydrogen bonds and their B3LYP calculated values are equal to -525 and -421 cm^{-1} for dSS1 and dSS3, respectively. In Table 3, the calculated and the experimental ΔνOH and ΔνC=O shifts are compared for the most stable dimer structures. The remaining data are shown in Table S3 (Supplementary data).

Table 3. The calculated harmonic (scaled) wavenumber shifts Δν (cm^{-1}) and intensities I (km mol^{-1}) of the most stable dSSn dimers compared to the experimental shifts. The corresponding monomer data are also given.

dSS1[a]			dSS2			dSS3			Ar matrix		SSC monomer		
	$\Delta\nu^{b}$	I		Δν	I		Δν	I		Δν		ν_{theor}	ν_{exp}
νOH_{ANs1}	+14	65	νOH_{CBs}	-2	39	νOH_{CN}	-2	90		-111, -117, -131	νOH_{C}	3573	3561
νOH_{ANs2}	+14	88	νOH_{CBas}	-2	95	νOH_{AN}	-11	88	νOH	-373			
νOH_{CBas}	-525	3318	νOH_{ABs}	-78	1043	νOH_{AB}	-53	111			νOH_{A}	3562	3561
νOH_{CBs}	-622	0	νOH_{ABas}	-98	62	νOH_{CB}	-421	1264		-399			
$\nu C{=}O_{Bas}$	-56	715	$\nu C{=}O_{Bas}$	-9	766	$\nu C{=}O_{N}$	-5	325		$-16/-12_{sh}$			
									νC=O	-41	νC=O	1773	1773
$\nu C{=}O_{Bs}$	-105	0	$\nu C{=}O_{Bs}$	-16	63	$\nu C{=}O_{B}$	-39	268		$-54/-56_{sh}$			

[a] ν – stretching, s – symmetric, as – asymmetric, A – alcohol group, C – carboxylic group, B – bonded, N – nonbonded, sh-shoulder, theor – theoretical, exp – experimental

[b] Scaling factors equal to 0.9506 and 0.9845 above and below 2500 cm^{-1}, respectively.

The second set of bands in the νOH region at 3450, 3444 and 3430 cm^{-1} is characterized by much smaller wavenumber shifts of -111, -117 and -131 cm^{-1}. There are three dimer structures (dSS2, dSS5 and dSS6) with the calculated ΔνOH shifts, which are reasonable close to the experimental values. However two of them (dSS5 and dSS6) have to be excluded due to the fact that they are characterized theoretically by relatively intense blue-

shifted νC=O bands as compared to the monomer band (see Table S3) but this is not what is observed experimentally. Therefore, the only possible structure to explain the appearance of the νOH bands in question is dSS2 dimer. Possible explanation of the observed multiple structure of the absorption at ca. 3440 cm^{-1} could be matrix site effect.

Further analysis of the dimer structures present in argon matrices was performed based on the νC=O stretching region (Fig. 4). Two dimer bands with the pronounced shoulders are observed below the νC=O monomer absorption at 1757/1761sh and 1719/1717sh cm^{-1}. There is also an additional broad band with a maximum at 1733 cm^{-1} (see Fig. 4). The corresponding ΔνC=O shifts are equal to -16/-12, -54/-56 and -41 cm^{-1}, respectively relative to the monomer band at 1773 cm^{-1}. Since the strongest red shift of the C=O stretch among all dimer species was computed for the dSS1 form (-56 cm^{-1}) the absorption at 1719/1717 cm^{-1} may be assigned to this cyclic structure with the experimental shifts equal to -54/-56 cm^{-1}. Two remaining dimer species (dSS2 and dSS3) are characterized by predicted weaker perturbation of the νC=O mode with the values of -9 and -16 cm^{-1} (dSS2) and -5 and -39 cm^{-1} (dSS3). The 1733 cm^{-1} band (ΔνCO = -41 cm^{-1}) is assigned to the dSS3 dimer due to the very good agreement with the predicted shift. In turn both dSS2 and dSS3 may contribute to the 1760 cm^{-1} absorption characterized by the weakest perturbation of the νC=O mode (-13/-16 cm^{-1}, see Fig. 4).

4. Conclusions

Based on the experimental findings and the spectral assignment supported by the theoretical calculations, the dimers of glycolic acid were observed and characterized for the first time. Based on the ΔνOH and ΔνC=O shifts the three most stable species (dSS1, dSS2 and dSS3) were identified in annealed matrices. All of them are cyclic structures with two O-H···O hydrogen bonds formed between two carboxylic groups (dSS1), between alcohol OH groups interacting with the oxygen atoms of the carbonyl groups (dSS2) and with one O-

H···O and one C-H···O bonds (dSS3). The observed linear correlation between the absorption intensities of monomer and the annealing products pointed out that dimerization was the major loss channel of monomers and other formation channels than dimerization were negligible.

ACKNOWLEDGMENT

The research was supported by the National Science Centre Project No. 2013/11/B/ST4/00500 (at UWr) and Academy of Finland Project No. 286844 (at JYU). J. A. gratefully acknowledges the research period system and the mobility funding of the University of Jyväskylä. A grant of computer time from the Wrocław Center for Networking and Supercomputing is gratefully acknowledged.

Appendix A. Supplementary data

Supplementary data related to this article can be found at https://....

References

[1] W. Klemperer, V. Vaida, *PNAS*, 103 (2006) 10584-10588.
[2] A.A. Vigasin, Z. Slanina (eds) "Molecular complexes in Earth's, planetary, cometary, and interstellar atmospheres" World Scientific Publishing Co. Pte. Ltd., Singapore, 1998.
[3] V. Vaida, Perspective: Water Cluster Mediated Atmospheric Chemistry, J. Chem. Phys.135 (2011) 02090 1-10.
[4] W. Sander, M. Gantenberg, Spectrochim. Acta, A 62 (2005) 902-909.
[5] F. Ito, J. Chem. Phys. 128 (2008) 114310 1-13.
[6] A. Olbert-Majkut, J. Ahokas, J. Lundell, M. Pettersson, Chem. Phys. Lett. 468 (2009) 176-183.
[7] A. Olbert-Majkut, J. Ahokas, J. Lundell, M. Pettersson, J. Raman Spectrosc. 42 (2011) 1670-1681.
[8] A. Olbert-Majkut, J. Lundell, M. Wierzejewska, J. Phys. Chem. A., 118 (2014) 350-357.
[9] A. Olbert-Majkut, M. Wierzejewska, J. Lundell, Chem. Phys. Lett. 616-617 (2014) 91-97.
[10] P.-G. Jönsson, Acta Crystallogr. B27 (1971) 893-898.
[11] J.L. Derissen, P.H. Smit, Acta Crystallogr. A33 (1977) 230-232.
[12] Z. Berkovitch-Yellin, L. Leiserowitz, J. Am. Chem. Soc. 104 (1982) 4052-4064.
[13] T. Beyer, S.L. Price, J. Phys. Chem. B 104 (2000) 2647-2655.
[14] A. Gavezzotti, J. Mol. Struct. 615 (2002) 5-12.
[15] X-Y. Zhang, W. Liu, W. Tang, Y-B. Lai, Acta Cryst. E63 (2007) o3764.
[16] M.Pagacz-Kostrzewa, D. Jesariew, M. Podruczna, M. Wierzejewska, Spectrochim. Acta A 108 (2013) 229-235.
[17] C.E. Blom, A. Bauder, J. Am. Chem. Soc. 104 (1982) 2993-2996.
[18] H. Hasegawa, O. Ohashi, I. Yamaguchi, J. Mol. Struct. 82 (1982) 205-211.
[19] D.K. Havey, K. J. Feierabend, V. Vaida, J. Phys. Chem. A 108 (2004) 9069-9073.
[20] D.K. Havey, K. J. Feierabend, K. Takahashi, R.T. Skodje, V. Vaida, J. Phys. Chem. A 110 (2006) 6439-6446.

[21] H. Hollenstein, R. W. Schär, N. Schwizgebel, G. Grassi, H. H. Günthard, Spectrochim. Acta Part A Mol. Spectrosc. 39 (1983) 193-213.
[22] H. Hollenstein, T. K. Ha, H. H. Günthard, J. Mol. Struct. 146 (1986) 289-307.
[23] I.D. Reva, S. Jarmelo, L. Lapinski, R. Fausto, J. Phys. Chem. A 108 (2004) 6982-6989.
[24] I.D. Reva, S. Jarmelo, L. Lapinski, R. Fausto, Chem. Phys. Lett. 389 (2004) 68-74.
[25] A. Halasa, L. Lapinski, I. Reva, H. Rostkowska, R. Fausto, M.J. Nowak, J. Phys. Chem. A 118 (2014) 5626-5635.
[26] P.D. Godfrey, F.M. Rodgers, R.D. Brown, J. Am. Chem. Soc. 119 (1997) 2232-2239.
[27] A.J. Barnes, J. Mol. Struct. 100 (1983) 259-280.
[28] A.J. Barnes, Z. Mielke, J. Mol. Struct. 1023 (2012) 216-221.
[29] M.J. Almond, N. Goldberg, Annu. Rep. Prog. Chem. Sect. C, 103 (2007) 79-133.
[30] M.J. Frisch, G.W. Trucks, H.B. Schlegel, G.E. Scuseria, M.A. Robb, J.R. Cheeseman, G. Scalmani, V. Barone, B. Mennucci, G.A. Petersson, H. Nakatsuji, M. Caricato, X. Li, H.P. Hratchian, A.F. Izmaylov, J. Bloino, G. Zheng, J.L. Sonnenberg, M. Hada, M. Ehara, K. Toyota, R. Fukuda, J. Hasegawa, M. Ishida, T. Nakajima, Y. Honda, O. Kitao, H. Nakai, T. Vreven, J.A. Montgomery, Jr., J.E. Peralta, F. Ogliaro, M. Bearpark, J.J. Heyd, E. Brothers, K.N. Kudin, V.N. Staroverov, R. Kobayashi, J. Normand, K. Raghavachari, A. Rendell, J.C. Burant, S.S. Iyengar, J. Tomasi, M. Cossi, N. Rega, J.M. Millam, M. Klene, J.E. Knox, J.B. Cross, V. Bakken, C. Adamo, J. Jaramillo, R. Gomperts, R.E. Stratmann, O. Yazyev, A.J. Austin, R. Cammi, C. Pomelli, J.W. Ochterski, R.L. Martin, K. Morokuma, V.G. Zakrzewski, G.A. Voth, P. Salvador, J.J. Dannenberg, S. Dapprich, A.D. Daniels, Ö. Farkas, J.B. Foresman, J.V. Ortiz, J. Cioslowski, D.J. Fox, Gaussian 09, Revision E.01, Gaussian Inc., Wallingford CT, 2009.
[31] M. J. Frisch, M. Head-Gordon, J. A. Pople, Chem. Phys. Lett., 166 (1990) 275-80.
[32] M. J. Frisch, M. Head-Gordon, J. A. Pople, Chem. Phys. Lett., 166 (1990) 281-89.
[33] M. Head-Gordon, J. A. Pople, M. J. Frisch, Chem. Phys. Lett., 153 (1988) 503-06.
[34] S. Saebø, J. Almlöf, Chem. Phys. Lett., 154 (1989) 83-89.
[35] M. Head-Gordon, T. Head-Gordon, Chem. Phys. Lett., 220 (1994) 122-28.
[36] A.D. Becke, Phys. Rev. A At. Mol. Opt. Phys. 38 (1988) 3098–3100
[37] S. Grimme, J. Antony, S. Ehrlich, S. Krieg, J. Chem. Phys. 132 (2010) 154104.
[38] L. Goerigk, S. Grimme, J. Chem. Theory Comput. 7 (2011) 291-309.
[39] S. Grimme, S. Ehrlich, L. Goerigk, J. Comp. Chem. 32 (2011) 1456-65.
[40] S. Grimme, J. Chem. Phys. 124 (2006) 034108.
[41] C. Lee, W. Yang, R.G. Parr, Phys. Rev. B. Condens. Matter. 37 (1988) 785–789.
[42] A.D. Becke, J. Chem. Phys. 98 (1993) 5648–5652.
[43] S.F. Boys, F. Bernardi, Mol. Phys. 19 (1970) 553-566.
[44] R.F. Bader, Atoms In Molecules: A Quantum Theory, Oxford University Press, New York, 1990.

Highlights

- Structure of glycolic acid dimers present in solid Ar was studied by FTIR spectroscopy
- MP2 and DFT calculations revealed 27 stable dimer structures
- Comparison of the experiment and theory allowed to identify the most stable species